Journal of Inorganic and General Chemistry
ZAAC
Zeitschrift für anorganische und allgemeine Chemie
DOI: 10.1002/zaac.202000039
ARTICLE

Influences of Steric Factors on the Reactivity and Structure of Diorganoalkoxysilylamides

Lukas Zibula,[a] Moritz Achternbosch,[a] Jonathan Wattenberg,[a] Felix Otte,[a] and Carsten Strohmann*[a]

Dedicated to Prof. Dr. Manfred Scheer on the Occasion of his 65th Birthday

Abstract. The combination of an alkoxy and an amino function combined in one silane is rarely found due to the difficult synthesis and isolation.[1] However, this combination offers unique opportunities to investigate the influence of steric requirements or the size of a metal on the structure or reactivity of alkoxysilylamides towards electrophiles by varying the metallating reagent (*n*-butyllithium or di-*n*-butylmagnesium) or the organo group on the amino function. For this purpose, we synthesized two alkoxyaminosilanes with acidic NH units that can be metalated. On the one hand, the *tert*-butylamino-substituted (*tert*-butylamino)-methoxydiphenylsilane (**1**) and on the other hand the *iso*propylamino-substituted methoxydiphenyl(*iso*propylamino)silane (**2**). The resulting structures showed an interesting interrelation between the Si–O or Si–N bond lengths and the strength of the coordinative bond to the corresponding metal cation (lithium or magnesium).

Introduction

Alkoxy- (**A**) and aminosilanes (**B**) are two of the most popular silylation reagents in molecular and material chemistry (e.g. silylation of surface-bound silanol groups).[2] On the other hand, there are only a few representatives in which both functions (alkoxy- and amino-function) are combined in one compound (**C**).[1] This is due to the inefficient and difficult synthesis via commonly used chlorosilanes, which results in undesired multiple substitutions. The few existing representatives of the alkoxy-aminosilanes (**C**) are limited to sterically demanding organic substituents on alkoxy and amino function (Figure 1).[1]

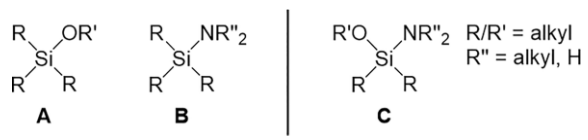

Figure 1. Structural formula of an alkoxy-, amino- and alkoxyaminosilane.

Studies on sterically less demanding organyl groups have so far been lacking. In addition to the large capability in surface modification, alkoxyaminosilanes have a great potential as chelate ligands with different metals, which has already been shown in different publications,[1a–1c] but only in their bulky form. For this reason, we were interested in extending the few existing studies on bulky alkoxyaminosilanes (**C**) and their metallated derivatives to sterically less demanding silanes and in investigating the influence of steric effects and different metals on structure and reactivity.

In order to reduce the steric demands compared to compounds known from the literature, we have replaced the bulky alkoxy function with a methoxy function. As an example molecule we used the literature-known methoxydiphenyl(*iso*propylamino)-silane (**2**), which can be prepared according to *Sakaba* et al. using the corresponding chloromethoxysilane precursor.[1d] We herein describe our first results concerning the reaction of methoxyaminosilanes with metalating reagents, such as *n*-butyllithium and di-*n*-butylmagnesium, which led to interesting structural motifs. DFT calculations also provide further insight into the observed structural changes depending on the steric demand or the choice of metal.

Results and Discussion

The alkoxyaminosilane methoxydiphenyl(*iso*propylamino) silane (**2**) can be prepared according to *Sakaba* et al. by the reaction of chloromethoxydiphenylsilane (**3**) with *iso*propylamine (**4**).[1d] It was possible to obtain crystals that were suitable for single-crystal X-ray diffraction analysis. Compound **2** crystallized from *n*-hexane in the form of colorless platelets at –80 °C in the monoclinic crystal system in space group $P2_1/n$.

Scheme 1 shows the asymmetric unit of the structure in the solid state of compound **2**. Both the Si–O [1.6550(10) Å] and the Si–N distance [1.6866(11) Å] correspond to typical bond lengths for the compound class of alkoxyaminosilanes.[1a–1c,1g] The short Si–N distance also shows the high ionic character of an Si–N bond. As expected, the nitrogen has a trigonal planar

* Prof. Dr. C. Strohmann
E-Mail: carsten.strohmann@tu-dortmund.de
[a] Institute of Inorganic Chemistry
TU Dortmund University
Otto-Hahn-Str. 6
44227 Dortmund, Germany
Supporting information for this article is available on the WWW under **http://dx.doi.org/10.1002/zaac.202000039** or from the author.

geometry with an angle sum of 359.96°, which corresponds to expected sp^2 hybridization. The sum of the angles also agrees with comparable representatives of this class of compounds known from the literature.[1a–1c,1g] In order to investigate the steric influences on the structure of the metal derivatives, (*tert*-butylamino)methoxydiphenylsilane (**1**) was also prepared using the analogue synthesis route with *tert*-butylamine (**5**).[1d] Compound **1** crystallized from *n*-pentane in the form of colorless platelets at –80 °C in the orthorhombic crystal system in space group $Pca2_1$.

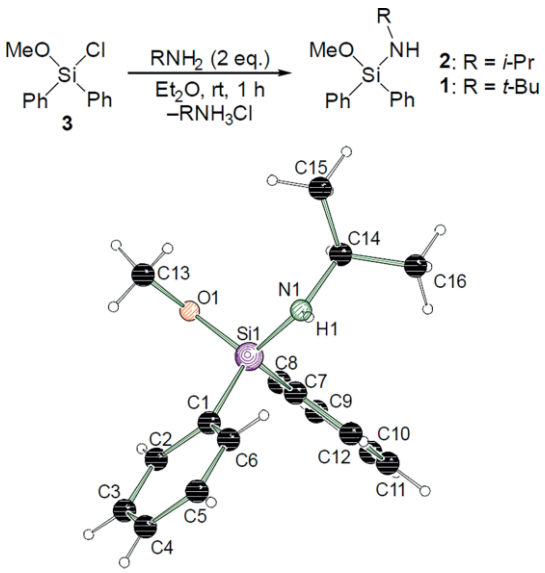

Scheme 1. Molecular structure in the crystal with selected bond lengths /Å and angles /° of **2**: Si1–O1 1.6550(10), Si1–N1 1.6866(11), Si1–C1 1.8657(13), Si1–C7 1.8687(13), N1–H1 0.880(19), N1–C14 1.4681(15), O1–C13 1.4297(16), Si1–O1–C13 119.76(9), N1–Si1–C1 109.40(6), O1–Si1–N1 112.52(5), Si1–N1–H1 125.1(11), C14–N1–H1 112.4(11), Si1–N1–C14 122.46(9).

The asymmetric unit contains two molecules with the same atomic connectivity, but only one has been shown in Figure 2 for a better overview. Due to the moderate quality of the data sets, only the atomic connectivity can be discussed. However, it can be assumed that a trigonal-planar geometry at the nitrogen center also prevails here, since the atomic connectivity of the structure obtained can be described as analogous to that of compound **2**.

Subsequently, the alkoxyaminosilanes **1** and **2** with an acidic NH unit were solved in THF and treated with *n*-butyllithium (Scheme 2). The molecular structures of the resulting deprotonated dimeric lithium derivatives **6** and **7** are shown in Figure 3. Compound **6** (Figure 3a) crystallizes at room temperature from THF in the form of colorless blocks in the monoclinic crystal system in the space group $P2_1/n$. The asymmetric unit contains half of the shown dimer. The lithium atom is coordinated by a THF solvent molecule and the nitrogen as well as the oxygen of the silane. The nitrogen atom coordinates both lithium centers of the dimer, which results in a coordination number of four for the lithium cation.

This coordination pattern, with three fused four-membered rings, spans a ladder-structure, which matches with the known

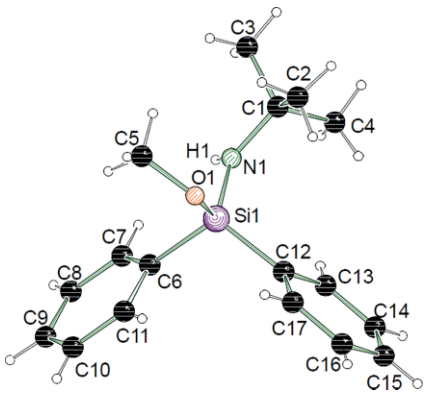

Figure 2. Molecular structure in the crystal with selected bond lengths /Å and angles /° of **1**: Twin law: –1, 0, 0; 0, –1, 0; 0, 0, –1. Si1–O1 1.651(4), Si1–N1 1.703(4), Si1–C6 1.871(5), Si1–C12 1.861(6), N1–Si1–O1 113.5(2), O1–Si1–C6 107.5(2), O1–Si1–C12 102.6(2), N1–Si1–C6 108.0(2), N1–Si1–C12 115.1(2), C6–Si1–C12 109.9(2). More information can be found in the Supporting Information.

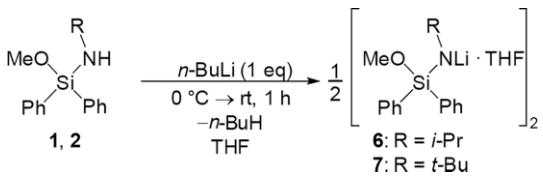

Scheme 2. Lithiation of the alkoxyaminosilanes **1** and **2**.

bulkier structures from *Veith* et al.[1a–1c] The shortening of the Si–N bond [1.663(2) Å] can be observed because of the increased charge density on nitrogen due to the deprotonation. This goes in hand with an extension of the Si–O bond [1.6791(16) Å]. This can be explained by the interaction of single oxygen- or nitrogen-functions in alkoxy- or aminosilanes with silicon, which has already been described in the literature.[3] The increased charge density on the nitrogen also increases the strength of the interaction between silicon and nitrogen. This in turn reduces the interaction strength between oxygen and silicon. In addition, the oxygen also interacts with the lithium cation, which would explain the lengthening of the Si–O bond. However, if the steric demand on the amine group is increased to a *tert*-butyl group, the structural motif changes from a ladder- to a bowl-shape (Figure 3b). The dimeric lithium derivative **7** crystallized at –80 °C from THF in the form of colorless prisms in the monoclinic crystal system in the space group *C*2/*c*. The asymmetric unit contains half of the dimer shown in Figure 3b. The atomic connectivity is analogous to **6**, so that the three annealed four-membered rings can also be found in the molecular structure of **7**, but here the two outer rings are on the same side. That leads to a structural motif change from a ladder structure in **6** to a bowl structure in **7**. The bond lengths Si1–N1 [1.6682(5) Å], Si1–O1 [1.6784(5) Å], Si1–C1 [1.8902(6) Å], Si1–C7 [1.8925(6) Å] and N1–Li1^{i} [2.0872(13) Å] are all comparable to the structure of **6**. Only the N1–Li1 distance is significantly longer [2.1755(13) Å], which can be attributed to steric overload.

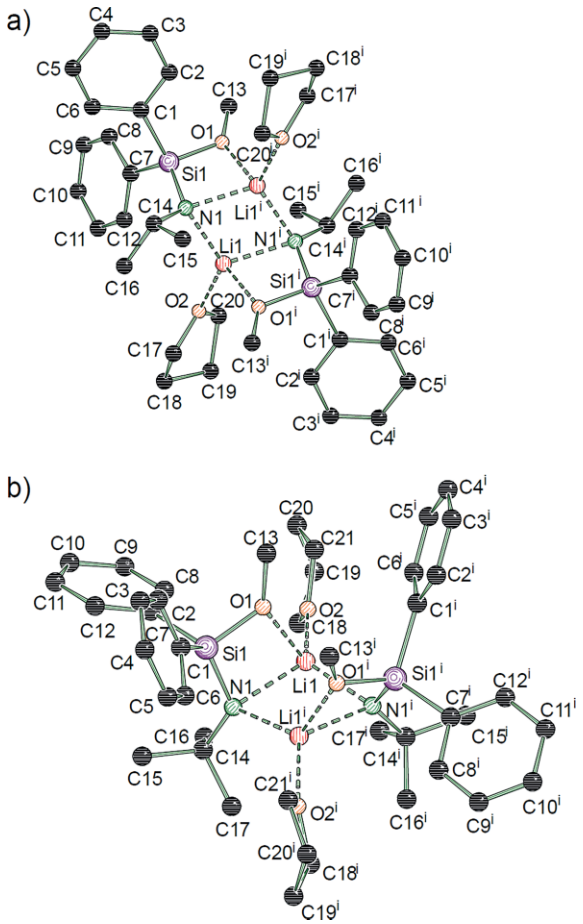

Figure 3. Molecular structure in the crystal (hydrogen atoms and disorders are omitted for clarity) with selected bond lengths /Å and angles /° of (a) **6**: Symmetry operations: i = 1 –*x*, 1 –*y*, 1 –*z*. Si1–N1 1.663(2), Si1–O1 1.6791(16), Si1–C1 1.891(2), Si1–C7 1.897(2), N1–Li1 2.043(4), N1–Li1^{i} 2.119(4), O1–Li1^{i} 2.082(4), O2–Li1 1.986(4), O1–Si1–N1 100.55(9), Si1–O1–Li1^{i} 91.49(13), O1^{i}–Li1–N1^{i} 75.46(16), Si1–N1–Li1^{i} 90.66(14), N1–Li1–N1^{i} 106.87(18), Li1–N1–Li1^{i} 73.13(18); (b) **7**: Symmetry operations: i = 1–x, y, 0.5–z. Si1–N1 1.6682(5), Si1–O1 1.6784(5), Si1–C1 1.8902(6), Si1–C7 1.8925(6), N1–Li1 2.1755(13), N1–Li1^{i} 2.0872(13), O1–Li1 2.0449(13), O2–Li1 2.1249(13), N1–C14 1.4686(7), O1–Si1–N1 99.70(2), Si1–N1–Li1 89.30(4), N1–Li1–O1 74.54(4), Li1–O1–Si1 93.58(4), Li1–N1–Li1^{i} 74.51(5), N1–Li1–N1^{i} 103.82(5).

In order to gain a better insight into this structural change by increasing sterics, DFT calculations were carried out at the M062X/6-31+g(d) level (Figure 4). These calculations show that the observed bowl-structure of **7** has a clear preference over the ladder structure with an energy difference of 28 kJ·mol^{-1}. If the phenyl groups are replaced by methyl groups, the thermodynamic situation changes towards the ladder structure, so that the ladder structure is favored with an energy difference of 7 kJ·mol^{-1}. That indicates that the observed bowl-structure of **7** is formed due to the repulsion between the *tert*-butyl- and the phenyl groups.[4] In addition to the structural differences between **6** and **7**, a change in the reactivity towards chlorotrimethylsilane (TMSCl) can also be observed (Scheme 3). The reaction of **2** with chlorotrimethylsilane resulted in the corresponding disilazane **8**. In the case of the *tert*-butylamino substituted alkoxyaminosilane **1**, no reaction with TMSCl can be observed even at high reaction temperatures in toluene. Here a steric overload around the nitrogen atom seems to occur, which kinetically prevents the reaction with TMSCl.

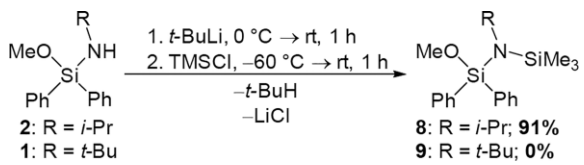

Scheme 3. Lithiation of the alkoxyaminosilanes **1** and **2** followed by the reaction with chlorotrimethylsilane (TMSCl).

We also wanted to investigate the influence of different metals on the structure. So we treated **2** with dibutylmagnesium instead of *n*-butyllithium, which resulted in the magnesium derivative shown in Scheme 4. The dimeric magnesium deriva-

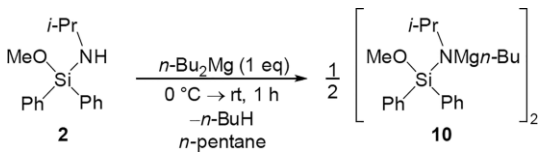

Scheme 4. Deprotonation of the alkoxyaminosilane **2** with di-*n*-butylmagnesium.

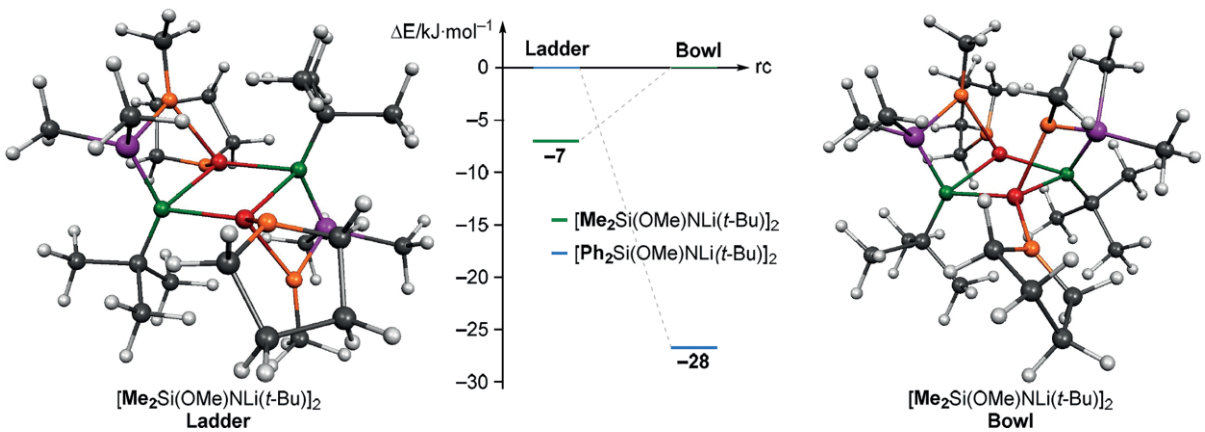

Figure 4. Energy profile for the two isomers [M062X / 6-31+g(d)].

tive **10** crystallized at –80 °C from *n*-pentane in the form of colorless blocks in the monoclinic crystal system in space group $P2_1/n$.

Due to the disorder of the *iso*propyl groups, which breaks the symmetry, the asymmetric unit contains the entire dimeric compound shown in Figure 5. The bowl structure seen is formed by three fused four-membered rings, which are made up of two magnesium cations, two aminomethoxysilanes and two butyl ligands. In comparison to the lithium derivative **6**, with the atom connectivity remaining the same, the structural motif is changed from a ladder structure (Li) to a bowl structure (Mg) by changing the metal cation. All bond lengths and angles are comparable to known magnesium derivative structures of aminosilanes.[5] However, compared to the lithium structure **6**, both the Si1–O1 [1.6906(13) Å] as well as the Si1–N1 [1.6981(16) Å] bond lengthens. One explanation for this could be the stronger interaction of the two donor atoms with the formally doubly charged magnesium cation, which in turn reduces the attractive interaction of the two functions with the central silicon atom.[3]

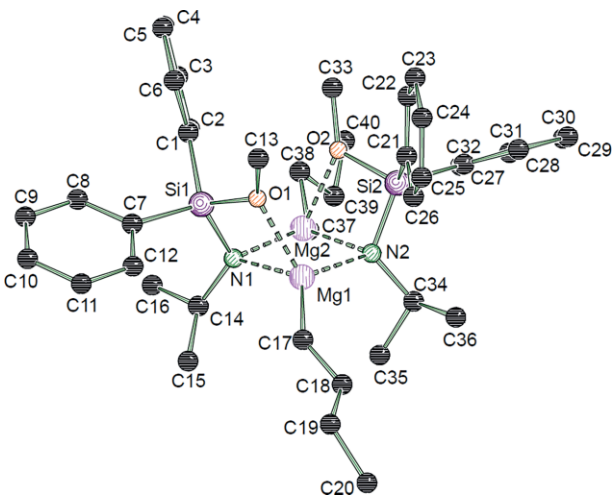

Figure 5. Molecular structure in the crystal (hydrogen atoms and disorders are omitted for clarity) with selected bond lengths /Å and angles /° of **10**: Si1–N1 1.6981(16), Si2–N2 1.6993(17), Si1–O1 1.6906(13), Si2–O2 1.6896(14), Si1–C1 1.866(2), Si1–C7 1.8666(19), Si2–C21 1.877(2), Si2–C27 1.8670(19), N1–Mg1 2.1733(16), N1–Mg2 2.1156(16), N2–Mg1 2.1100(16), N2–Mg2 2.1801(16), O1–Mg1 2.1183(14), O2–Mg2 2.1252(14), N2–C34 1.478(3), N1–C14 1.492(2), Mg1–C17 2.123(2), Mg2–C37 2.145(9), O1–Si1–N1 96.30(7), Si1–N1–Mg1 93.26(7), N1–Mg1–O1 72.04(6), Mg1–N1–Mg2 86.54(6), N1–Mg2–N2 93.15(6), Si1–N1–C14 119.43(12).

Conclusions

In the course of our investigations on metallation reactions of alkoxyaminosilanes, it was possible to obtain three N-metallated products. These could be analyzed using single-crystal X-ray diffraction analysis and had different structural motifs depending on the used metal alkyl or the steric demand of the silane. It was shown that the obtained lithium and magnesium derivatives form a dimeric structure in the solid, which results from three fused four-membered rings. However, the arrangement of these rings depends on the metal or the steric demand of the organo function at the nitrogen center. In the case of lithium derivatives with lower steric demand on the amino function, a ladder structure motif is adopted, whereas in the case of the *tert*butyl-substituted nitrogen center or in the case of magnesium derivatives, a bowl structure is adopted. An interplay of the Si–N and Si–O interactions could also be observed. The increased charge density on the deprotonated aminofunction in compound **6** and the associated stronger interaction with the central silicon atom results in an extension of the Si–O bond. Based on these experimentally obtained results, quantum chemical calculations showed that the repulsion of the organyl groups on silicon and nitrogen leads to a favoring of the bowl structure (**7**). However, if the steric demand is reduced, the thermodynamic situation is reversed and the observed ladder structure appears to be more stable.

In addition, a change in the reactivity between the two investigated lithiated model compounds **6** and **7** towards electrophiles was also found. While the lithiated *iso*propylamino substituted silane **6** reacts with TMSCl with good yields, no formation of the corresponding disilazane can be observed in the analogous *tert*-butylamino substituted case (**7**). The combination of alkoxy and amino functions in one silane proves to be an interesting class of compounds for investigating the steric influence on reactivity and structure and the interplay between multiple donor atoms in a organosilane. The challenge for the future will be the development of an effective synthesis method for the preparation of alkoxyaminosilanes regardless of steric demand.

Experimental Section

General Considerations: All preparations were performed in dried, oxygen-free solvents under an inert gas atmosphere of argon. The standard glass equipment was flame dried in an evacuated state before working with the oxygen or moisture-sensitive compounds.

Characterization: The NMR spectra were recorded with a Bruker Avance III HD spectrometer (T = 300 K) with δ referenced to external tetramethylsilane (^{1}H, ^{13}C and ^{29}Si). ^{1}H and ^{13}C NMR spectra were calibrated by using the solvent residual peak [C_6D_5H: $\delta(^1H)$ = 7.16 ppm] and the solvent peak [C_6D_6: $\delta(^{13}C)$ = 128.4 ppm], respectively. ^{29}Si NMR spectra were calibrated by using tetramethylsilane [$Si(CH_3)_4$: $\delta(^{29}Si)$ = 0.0 ppm]. All ^{29}Si NMR spectra were recorded using the INEPT method and thus appear in the form of refocused singlet signals without signal splitting by scalar coupling ({1H}). Elemental analysis was performed with a Vario MICRO cube from Elementar. The proportions of the respective elements were given in percent. Gas Chromatograph: Model 7890B from Agilent; HP-5 MS capillary column from Agilent (length 30 m, ID 0.25 mm); Carrier gas helium. The temperature programs used are specified. EI-MS: Mass Selective Detector 5977A from Agilent (electron impact ionization, 70 eV). The *m*/*z* values of the molecular ions and the selected fragment ions are based in each case on the mass numbers of the isotopes with the greatest natural frequency (^{1}H, ^{12}C, ^{14}N, ^{16}O, ^{28}Si).

The single-crystal X-ray diffraction data was collected with a Bruker D8 Venture four-circle diffractometer from Bruker AXS GmbH. Area counter CMOS detector used: Photon100 from Bruker AXS GmbH (**1**); CPAD detector used: Photon II from Bruker AXS GmbH (**2**, **6**, **7**,

Table 1. Most important crystal data and structure refinement for compound **1**, **2**, **6**, **7**, **10**.

	1 [a]	**2**	**6**	**7**	**10** [b]
Empirical formula	$C_{17}H_{23}NOSi$	$C_{16}H_{21}NOSi$	$C_{40}H_{56}Li_2N_2O_4Si_2$	$C_{42}H_{60}Li_2N_2O_4Si_2$	$C_{40}H_{58}Mg_2N_2O_2Si_2$
Formula weight	285.45	271.43	698.92	726.98	703.68
Crystal system	orthorhombic	monoclinic	monoclinic	monoclinic	monoclinic
Space group	$Pca2_1$	$P2_1/n$	$P2_1/n$	$C2/c$	$P2_1/n$
a /Å	28.5610(16)	9.6211(12)	9.6986(19)	24.8655(13)	11.5715(15)
b /Å	6.0976(4)	10.8544(16)	14.798(3)	10.9154(5)	15.1856(18)
c /Å	18.2555(10)	15.0757(19)	14.047(3)	19.2365(9)	25.977(4)
α /°	90	90	90	90	90
β /°	90	103.352(5)	101.728(8)	126.491(2)	90.089(5)
γ /°	90	90	90	90	90
Volume /Å^3	3179.3(3)	1531.8(4)	1973.9(6)	4197.5(4)	4564.7(10)
Z	8	4	2	4	4
ρ_{calc} /g·cm^{-3}	1.193	1.177	1.176	1.150	1.024
μ /mm^{-1}	0.144	0.146	0.131	0.125	0.136
F(000)	1232.0	584.0	752.0	1568.0	1520.0
2Θ range /°	4.462 to 52.996	4.668 to 64.996	5.096 to 53.992	4.252 to 69.998	4.126 to 56.758
R_{int}	0.0415	0.0539	0.0530	0.0315	0.0545
Goodness-of-fit on F^2	1.043	1.086	1.036	1.053	1.110
R [I ≥ 2σ (I)]	R_1 = 0.0757, wR_2 = 0.1813	R_1 = 0.0469, wR_2 = 0.1238	R_1 = 0.0601, wR_2 = 0.1420	R_1 = 0.0353, wR_2 = 0.0948	R_1 = 0.0572, wR_2 = 0.1524
wR (all data)	R_1 = 0.0873, wR_2 = 0.1938	R_1 = 0.0586, wR_2 = 0.1306	R_1 = 0.0750, wR_2 = 0.1556	R_1 = 0.0426, wR_2 = 0.1006	R_1 = 0.0647, wR_2 = 0.1568
$\Delta\rho$ (min, max) /e·Å^{-3}	2.79/–0.47	0.44/–0.34	0.95/–0.51	0.47/–0.26	0.46/–0.43

a) Twin refinement with HKLF4 data [twin law (–1, 0, 0; 0, –1, 0; 0, 0, –1)]. b) Twin refinement with HKLF4 data [twin law (1, 0, 0; 0, –1, 0; 0, 0, –1)].

10); X-ray sources: *IμS* Cu or Mo microfocus source from Incoatec GmbH with HELIOS mirror optics and single-hole collimator from Bruker AXS GmbH. Programs used for data collection: APEX3 Suite v2018.7–0 and integrated programs SAINT (integration) and SADABS (absorption correction) from Bruker AXS GmbH. The crystal structures were solved with the SHELXT program, the structure refinement with SHELXL.[6] The processing and finalization of the crystal structure data was carried out with the OLEX^2 program.[7] Non-hydrogen atoms were refined with anisotropic displacement parameters and hydrogen atoms isotropically on calculated positions using a riding model, except for the nitrogen bonded hydrogen of compound **2** which was located in a difference Fourier synthesis map and freely refined. Disorders in structure **6** and **10** were treated either with a fixed value or with a free variable. More details can be found in the Supporting Information. Crystallographic data and structure refinement results are summarized in Table 1.

Crystallographic data (excluding structure factors) for the structures in this paper have been deposited with the Cambridge Crystallographic Data Centre, CCDC, 12 Union Road, Cambridge CB21EZ, UK. Copies of the data can be obtained free of charge on quoting the depository numbers CCDC-1979658 for 1, CCDC-1979657 for 2, CCDC-1979659 for **6**, CCDC-1979660 for **7** and CCDC-1979661 for **10** (Fax: +44-1223-336-033; E-Mail: deposit@ccdc.cam.ac.uk, http://www.ccdc.cam.ac.uk).

The X-TEMP 2 system in combination with an SMZ1270 stereo microscope from Nikon Metrology GmbH was used for the selection of air and moisture sensitive crystals.[8] MicroMounts, MicroLoops or MicroGrippers from MiTeGen were used for the assembly.

Quantum Chemical Calculations: The quantum chemical calculations were carried out with the Gaussian version G016 revision B.01 program, and the molecular coordination was previously created using GaussView.[9] All energies were converted taking into account the zero point corrections (ZPE) obtained at the same level and stated in kJ·mol^{-1}. The ground state structures shown have been optimized without symmetry restrictions. A subsequent frequency calculation did not provide any imaginary frequencies for the minimum structures; exactly one imaginary frequency was available for transition states. For reasons of clarity, most of the energy-optimized structures were visualized in the form of Lewis formulas. The program Molekel V. 4.3 was used to record the three-dimensional arrangement.[10]

***t*BuHNSiPh$_2$(OMe) and *i*PrHNSiPh$_2$(OMe):** **1** and **2** were prepared according to published procedures.[1d] A portion of the products was removed for the crystallization and dissolved in about 1 mL of *n*-hexane (for **2**) or *n*-pentane (for **1**). At –80 °C both compounds crystallized in the form of colorless platelets.

***t*BuHNSiPh$_2$(OMe) (1): ^{1}H-NMR:** (600 MHz, C_6D_6): δ = 1.13 [s, 12 H, NC(CH_3)$_3$], 1.52 (s, 1 H, N*H*), 3.56 (s, 3 H, OCH_3), 7.17–7.24 (m, 6 H, CH_{meta}, CH_{para}), 7.77–7.86 (m, 4 H, CH_{ortho}) ppm. **{^{1}H}^{13}C-NMR**: (150 MHz, C_6D_6): δ = 33.9 [s, 3C; NC(CH_3)$_3$], 50.1 [s, 1C; NC(CH_3)$_3$], 50.4 (s, 1C; OCH_3), 128.4 (s, 4C; CH_{meta}), 130.2 (s, 2C; CH_{para}), 135.7 (s, 4C; CH_{ortho}), 137.2 (s, 2C; CH_{ipso}) ppm. **{^{1}H}^{29}Si-NMR**: (120 MHz, C_6D_6): δ = –29.6 (s, 1Si; *Si*) ppm. **GC/EI-MS**: [80 °C (1 min) – 270 °C (5.5 min) with 40 °C·min^{-1}], (70 eV, t_R = 5.57 min): m/z = 270 [(M – Me)$^+$, 100 %], 213 [(M – *t*BuNH)$^+$, 96 %], 183 [(HSiPh$_2$)$^+$, 53 %], 105 [(SiPh)$^+$, 16 %], 59 [(SiOCH$_3$)$^+$, 8 %], 77 (Ph$^+$, 4 %). $C_{17}H_{23}NOSi$ (285.46 g·mol^{-1}): calcd. C 71.5, H 8.1, N 4.9 %; found C 71.2, H 8.2, N 4.9 %.

***i*PrHNSiPh$_2$(OMe) (2): ^{1}H-NMR**: 400 MHz, C_6D_6): δ = 0.98 [d, 6 H, 3JHH = 6.24 Hz; SiNCH(CH_3)$_2$], 1.24 (d, 1 H, $^3J_{HH}$ = 10.27 Hz; SiN*H*), 3.07–3.19 [dspt, 1 H, $^3J_{HH}$ = 6.24 Hz, 10.39 Hz; SiNC*H*(CH_3)$_2$], 3.55 (s, 3 H, SiOCH_3), 7.20–7.25 (m, 6 H, C$H_{meta,para}$), 7.79–7.83 (m, 4 H, CH_{ortho}) ppm. **{^{1}H}^{13}C-NMR**: (100 MHz, C_6D_6):

δ = 28.0 [s, 2C; SiNHCH(CH_3)$_2$], 43.5 [s, 1C; SiNHCH(CH_3)$_2$], 50.5 (s, 1C; SiOCH_3), 128.5 (s, 4C; C_{meta}), 130.4 (s, 2C; C_{para}), 135.7 (s, 4C; C_{ortho}), 135.9 (s, 2C; C_{ipso}) ppm. **{^{1}H}^{29}Si-NMR**: (80 MHz, C_6D_6): δ = –27.0 (s, 1Si; *Si*) ppm. **GC/EI-MS**: [80 °C (1 min) – 250 °C (5.5 min) with 10 °C·min^{-1}], (70 eV, t_R = 13.2 min): *m*/*z* = 271 [M$^+$, 2 %], 256 [(M – Me]$^+$, 100 %], 240 [(M – OMe]$^+$, 2 %], 213 [(Ph_2MeOSi)$^+$, 96 %], 183 [(Ph_2SiH)$^+$, 43 %], 77 (Ph$^+$, 3 %). $C_{16}H_{21}NOSi$ (271.44 g·mol^{-1}): calcd. C 70.8, H: 7.8, N: 5.2 %; found C 71.0, H 8.0, N: 5.4 %.

[*i*PrLiNSiPh$_2$(OMe)·THF]$_2$ (6): A solution of methoxydiphenyl(*iso*-propyl-amino)silane (**2**) (0.207 g, 0.763 mmol, 1 equiv.) in 2 mL THF was carefully covered with *n*-butyllithium (0.300 mL of a 2.5 M solution in *n*-hexane, 0.750 mmol, 1 equiv.) at 0 °C. The reaction solution was quickly thawed to room temperature and left to stand. Compound **6** crystallized in the form of colorless blocks by subsequent storage for 24 h at room temperature.

[*t*BuLiNSiPh$_2$(OMe)·THF]$_2$ (7): A solution of (*tert*-butylamino)-methoxydiphenylsilane (**1**) (0.217 g, 0.760 mmol, 1 equiv.) in 2 mL THF was carefully covered with *n*-butyllithium (0.280 mL of a 2.5 M solution in *n*-Hexane, 0.700 mmol, 0.9 equiv.) at 0 °C. The reaction solution was quickly thawed to room temperature and left to stand for 1 h, during that time compound **7** crystallized in the form of colorless blocks.

***i*PrTMSNSiPh$_2$(OMe) (8):** A solution of methoxydiphenyl(*iso*propyl-amino)silane (**8**) (0.503 g, 1.85 mmol, 1 equiv.) in 10 mL THF was treated with *tert*-butyllithium (1.20 mL of a 1.9 M solution in *n*-pentane, 2.28 mmol, 1.2 equiv.) at 0 °C. The reaction mixture was thawed to room temperature and stirred for 1 h. The reaction solution was then cooled down to –60 °C. Chlorotrimethylsilane (TMSCl) (0.332 g, 3.06 mmol, 1.65 equiv.) was added and the mixture was stirred at room temperature for 2 h. The volatile substances were removed under reduced pressure and the residue was dissolved in *n*-pentane. The insoluble constituents were then filtered off inertly and the volatile substances were again removed from the filtrate under reduced pressure. Purification by distillation (temperature: 175 °C, pressure: 7×10^{-1} mbar) gave compound **8** as a colorless viscous liquid (0.576 g, 1.68 mmol, 91 %).

***i*PrTMSNSiPh$_2$(OMe) (8): ^{1}H NMR** (400 MHz, C_6D_6): δ = 0.21 [s, 9 H, Si(CH_3)$_3$], 1.22 [d, 6 H, $^3J_{HH}$ = 6.72 Hz; SiNCH(CH_3)$_2$], 3.37 (s, 3 H, SiOCH_3), 3.45 (spt, 1 H, $^3J_{HH}$ = 6.72 Hz; SiNCHCH$_3$Ph), 7.21–7.26 (m, 6 H, CH_{meta}, CH_{para}), 7.79–7.81 (m, 4 H, CH_{ortho}) ppm. **{^{1}H}^{13}C NMR** (100 MHz, C_6D_6): δ = 3.5 [s, 3C, Si(CH_3)$_3$], 26.4 [s, 2C; SiNCH(CH_3)$_2$], 48.0 [s, 1C; SiNCH(CH$_3$)$_2$], 51.3 (s, 1C; SiOCH_3), 128.3 (s, 4C; $C_{arom.}$), 130.2 (s, 2C; C_{para}), 136.2 (s, 4C; $C_{arom.}$), 137.5 (s, 2C; C_{ipso}) ppm. **{^{1}H}^{29}Si NMR** (80 MHz, C_6D_6): δ = –19.9 (s, 1Si), 3.5 (s, 1Si) ppm. **GC/EI-MS** [80 °C (1 min) – 250 °C (5.5 min) with 10 °C·min^{-1}], (70 eV, t_R = 15.7 min): *m*/*z* = 328 [(M – Me]$^+$, 100 %], 312 [(M – OMe]$^+$, 1 %], 270 [(M – Me_3Si)$^+$, 1 %], 239 [(M – Me_3Si – OMe)$^+$, 1 %], 224 [(M–Me_3Si–OMe–Me)$^+$, 47 %], 183 [(Ph_2SiH)$^+$, 49 %], 73 [(Me_3Si)$^+$, 7 %]. $C_{19}H_{29}NOSi_2$ (343,62 g·mol^{-1}): calcd. C 66.4, H 8.5, N 4.1 %; found C 66.9, H 8.7, N 4.0 %.

[*i*PrMgNSiPh$_2$(OMe)·*n*Bu]$_2$ (10): A solution of methoxydiphenyl-(*iso*propylamino)silane (**2**) (0.207 g, 0.763 mmol, 1 equiv.) in 2 mL *n*-pentane was carefully covered with di-*n*-butylmagnesium (0.740 mL of a 1 M solution in *n*-heptane, 0.740 mmol, 1 equiv.) at 0 °C. The reaction solution was quickly thawed and then stored at room temperature, whereby compound **10** crystallized in the form of colorless blocks.

Supporting Information (see footnote on the first page of this article): Crystallographic details and NMR spectra are found in the Supporting Information.

Acknowledgements

Open access funding enabled and organized by Projekt DEAL.

Keywords: Alkoxysilane; Lithium; Magnesium; Silylamides; Aminosilane

References

[1] a) M. Veith, R. Rösler, *J. Organomet. Chem.* **1982**, *229*, 131–138; b) M. Veith, *Angew. Chem. Int. Ed. Engl.* **1987**, *26*, 1–14; c) M. Veith, J. Böhnlein, *Chem. Ber.* **1989**, *122*, 603–607; d) H. Sakaba, H. Tonosaki, K. Isozaki, E. Kwon, *Organometallics* **2015**, *34*, 1029–1037; e) G. L. Fondong, E. Y. Njua, L. Stahl, *J. Organomet. Chem.* **2015**, *776*, 129–135; f) O. Schmitz-DuMont, D. Merten, D. Eiding, *Z. Anorg. Allg. Chem.* **1963**, *319*, 362–374; g) J. O. Bauer, C. Strohmann, *Angew. Chem. Int. Ed.* **2014**, *53*, 720–724; h) J. O. Bauer, C. Strohmann, *Angew. Chem. Int. Ed.* **2014**, *53*, 8167–8171; i) J. O. Bauer, C. Strohmann, *Chem. Commun.* **2012**, *48*, 7212–7214; j) U. Wannagat, G. Bogedain, H. Hajibegli, H.-H. Moretto, *Monatsh. Chem.* **1990**, *121*, 865–874; k) U. Wannagat, K. Behmel, H. Wolf, H. Bürger, *Z. Anorg. Allg. Chem.* **1964**, *333*, 62–70; l) U. Wannagat, S. Klemke, *Monatsh. Chem.* **1979**, *110*, 1077–1088.

[2] a) R. Murugavel, M. Bhattacharjee, H. W. Roesky, *Appl. Organomet. Chem.* **1999**, *13*, 227–243; b) R. Murugavel, A. Voigt, M. G. Walawalkar, H. W. Roesky, *Chem. Rev.* **1996**, *96*, 2205–2236; c) D. B. Cordes, P. D. Lickiss, F. Rataboul, *Chem. Rev.* **2010**, *110*, 2081–2173; d) T. Kang, I. Jang, S. Oh, *Colloids Surf. A: Physicochem. Eng. Aspects* **2016**, *501*, 24–31; e) G. Barroso, Q. Li, R. K. Bordia, G. Motz, *J. Mater. Chem. A* **2019**, *7*, 1936–1963; f) F. Zhang, K. Sautter, A. M. Larsen, D. A. Findley, R. C. Davis, H. Samha, M. R. Linford, *J. Am. Chem. Soc.* **2010**, *132*, 14648–14654.

[3] a) F. Weinhold, R. West, *J. Am. Chem. Soc.* **2013**, *135*, 5762–5767; b) F. Weinhold, R. West, *Organometallics* **2011**, *30*, 5815–5824; c) S. Grabowsky, M. F. Hesse, C. Paulmann, P. Luger, J. Beckmann, *Inorg. Chem.* **2009**, *48*, 4384–4393; d) R. J. Gillespie, S. Johnson, *Inorg. Chem.* **1997**, *36*, 3031–3039; e) R. Neufeld, R. Michel, R. Herbst-Irmer, R. Schöne, D. Stalke, *Chem. Eur. J.* **2016**, *22*, 12340–12346.

[4] Calculations of compound **6** with a nitrogen-bonded *isopropyl* group show a slight favoring of the bowl structure with 3 kJ/mol, but no significant difference between the two conformers. However, this shows that the *tert*-butyl group has a significantly higher repulsion with the phenyl groups than the *isopropyl* group. Note that due to the many possible isomers, only one isomer of each conformer was calculated based on the solid structure of **6** (more details can be found in the Supporting Information).

[5] a) V. P. Colquhoun, B. C. Abele, C. Strohmann, *Organometallics* **2011**, *30*, 5408–5414; b) V. P. Colquhoun, C. Unkelbach, C. Strohmann, *Chem. Commun.* **2012**, *48*, 5034–5036; c) V. P. Colquhoun, C. Strohmann, *Dalton Trans.* **2012**, *41*, 1897–1902; d) P. Schüler, H. Görls, M. Westerhausen, *Dalton Trans.* **2019**, *48*, 8966–8975.

[6] G. M. Sheldrick, *Acta Crystallogr., Sect. A* **2008**, *64*, 112–122.

[7] O. V. Dolomanov, L. J. Bourhis, R. J. Gildea, J. A. K. Howard, H. Puschmann, *J. Appl. Crystallogr.* **2009**, *42*, 339–341.

[8] T. Kottke, D. Stalke, *J. Appl. Crystallogr.* **1993**, *26*, 615–619.

[9] M. J. Frisch, G. W. Trucks, H. B. Schlegel, G. E. Scuseria, M. A. Robb, J. R. Cheeseman, G. Scalmani, V. Barone, G. A. Petersson, H. Nakatsuji, X. Li, M. Caricato, A. V. Marenich, J. Bloino, B. G.

Janesko, R. Gomperts, B. Mennucci, H. P. Hratchian, J. V. Ortiz, A. F. Izmaylov, J. L. Sonnenberg, D. Williams-Young, F. Ding, F. Lipparini, F. Egidi, J. Goings, B. Peng, A. Petrone, T. Henderson, D. Ranasinghe, V. G. Zakrzewski, J. Gao, N. Rega, G. Zheng, W. Liang, M. Hada, M. Ehara, K. Toyota, R. Fukuda, J. Hasegawa, M. Ishida, T. Nakajima, Y. Honda, O. Kitao, H. Nakai, T. Vreven, K. Throssell, J. A. Montgomery Jr., J. E. Peralta, F. Ogliaro, M. J. Bearpark, J. J. Heyd, E. N. Brothers, K. N. Kudin, V. N. Staroverov, T. A. Keith, R. Kobayashi, J. Normand, K. Raghavachari, A. P. Rendell, J. C. Burant, S. S. Iyengar, J. Tomasi, M. Cossi, J. M. Millam, M. Klene, C. Adamo, R. Cammi, J. W. Ochterski, R. L. Martin, K. Morokuma, O. Farkas, J. B. Foresman, and D. J. Fox, *Gaussian 16*, *Revision B.01*, Gaussian, Inc., Wallingford CT, **2016**.

[10] P. Flükiger, H. P. Lüthi, S. Portmann, J. Weber, *MOLEKEL 4.3*, Swiss Center for Scientific Computing, Manno, **2000**.

Received: January 30, 2020

